CAPACITIVE ABSOLUTE PRESSURE SENSOR WITH INDEPENDENT ELECTRODE AND MEMBRANE SIZES FOR IMPROVED FRACTIONAL CAPACITANCE CHANGE

Chia-Fang Chiang[1], *Andrew B. Graham*[2], *Matthew W. Messana*[1], *J Provine*[1], *Daniela T. Buchman*[1], *Gary J. O'Brien*[2], *and Thomas W. Kenny*[1]
[1]Stanford University, Stanford, CA, USA
[2]Robert Bosch LLC, Research and Technology Center, Palo Alto, CA, USA

ABSTRACT

Unlike a traditional capacitive pressure sensor, which uses the entire deflectable diaphragm as the electrode, this paper proposes the use of reduced electrode area to increase the fractional capacitance change and reduce the device's sensitivity to package stresses. Therefore, in addition to the low temperature sensitivity inherent in capacitive sensing, the proposed pressure sensor helps relax signal conditioning requirements typically associated with capacitive sensor interface circuitry.

KEYWORDS

Capacitive pressure sensor, microfabrication, silicon seal

INTRODUCTION

Among the many microelectromechanical transducers, MEMS pressure sensors have been commercially available for several decades. The two major transduction mechanisms are piezoresistive sensing, which measures the change in resistance as a result of pressure-induced stress on a diaphragm, and capacitive sensing, which measures the capacitance change due to pressure variations between two electrodes [1], [2]. Although both sensing mechanisms utilize a diaphragm to convert the applied pressure into an electrical signal, they are fundamentally different. Piezoresistive pressure sensors measure a stress-induced resistance change, typically in localized regions of highest stress, while capacitive pressure sensors measure a change in capacitance across the entire diaphragm.

Piezoresistive pressure sensors are favored for many applications because of their inherent linearity and the simplicity of the corresponding interface circuit design. Without careful design, the accuracy of piezoresistive pressure sensors can be significantly affected by their temperature sensitivity [3]. Furthermore, the required placement of the piezoresistors at the points of highest stress can make these sensors extremely sensitive to package-induced stress [4], [5]. Both problems require extra calibration effort and clever compensation techniques to achieve accurate pressure measurement. Capacitive sensors can overcome these issues by locating electrodes away from areas of high stress, but traditional designs have problems of their own, including small transduction signals, increased nonlinearity, and susceptibility to external RF interference.

In this paper, we present a new design for a capacitive pressure sensor that includes the following key innovations:

1) reduced capacitive electrode area to increase the fractional capacitance change and reduce sensitivity to package stress;
2) ultra-clean sealing process for the reference cavity using an epitaxial silicon reactor;
3) front-side wafer processing for low-cost manufacturing using standard Bosch manufacturing processes [6];
4) electrical via to substrate, forming a complete Faraday cage around the sensing elements.

DEVICE DEVELOPMENT

Analysis

For a clamped circular diaphragm with small deflections, the deflection, w, at a given pressure, P, can be determined by [7]

$$w(r) = \frac{P \cdot (a^2 - r^2)^2}{64D} \tag{1}$$

where a is the diaphragm radius and r is the radial distance from the center of the diaphragm. The flexural rigidity, D, incorporates the diaphragm's thickness, h, Young's modulus, E, and Poisson ratio, v, as follows,

$$D = \frac{Eh^3}{12(1 - v^2)}. \tag{2}$$

The capacitance between the diaphragm (top electrode) and a fixed plate (bottom electrode) can be expressed as

$$C = \int_0^{2\pi} \int_0^b \frac{\varepsilon_0 \varepsilon_r \cdot r}{d_0 - w(r,\theta)} dr d\theta \tag{3}$$

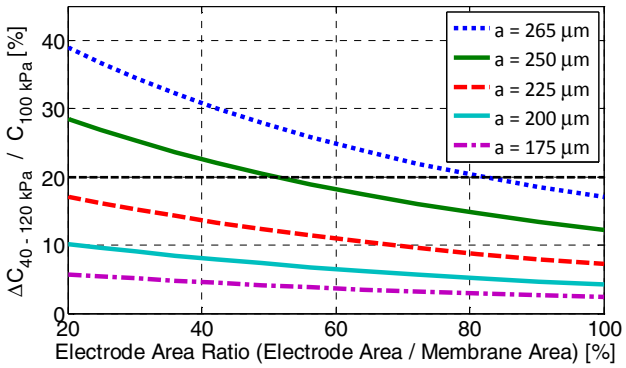

Figure 1: The effect of electrode size on $\Delta C/C_{nominal}$ for various diaphragm radius sizes. Data was simulated with diaphragm thickness $h=10\mu m$ and initial gap $d_0=1.5\mu m$.

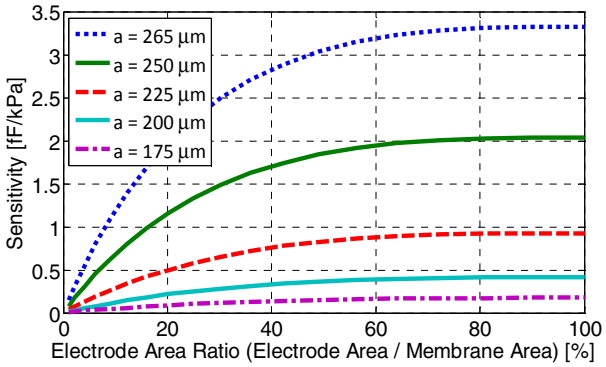

Figure 2: The effect of electrode size on sensitivity for various diaphragm sizes. Same simulation conditions as Figure 1.

where b is the electrode radius, d_0 is the initial gap between two counter electrodes, ε_0 is the permittivity of vacuum, and ε_r is the relative permittivity of the medium in the gap.

Based on the equations given above, a larger diaphragm leads to increased deflection, resulting in a larger capacitance change. However, given a fixed diaphragm thickness, large diaphragms are more susceptible to displacement due to temperature variations and stress-induced errors, which can jeopardize sensor performance. In order to improve sensing accuracy, a capacitive pressure sensor whose deformable electrode is represented by an electrically isolated and centrally located symmetric subset of the entire diaphragm is proposed. In order to better understand the features of such a pressure sensor, the effects of diaphragm and electrode sizes were investigated. It is clear from Figure 1 that decreasing the electrode size increases the relative capacitance change over the sensing range, denoted as $\Delta C/C_{nominal}$, where $C_{nominal}$ is measured at 101 kPa. In the case studied here, when the entire diaphragm is used as the electrode, $\Delta C/C_{nominal}$ is below 20%. Decreasing the electrode area improves this ratio, making the signal conditioning easier due to a larger relative capacitance change.

While it is desirable to have large $\Delta C/C_{nominal}$, there is also a trade-off with sensitivity. The plot of sensitivity versus electrode size in Figure 2 indicates that reducing the electrode area to 40% of the diaphragm area does not significantly sacrifice sensitivity because the capacitance change is concentrated primarily in the center of the diaphragm where maximum displacement occurs. However, further reduction of the electrode area leads to a quick drop in sensitivity, which is highly undesirable.

Fabrication

Structures were made using silicon-on-insulator (SOI) wafers, whose handle and device layers are both p-type silicon substrates. Electrode definition trenches are first etched using deep reactive-ion etching (DRIE). This defines the electrode size within the diaphragm. The trenches are then refilled with silicon nitride via low pressure chemical vapor deposition (LPCVD). Deposition conditions are set to achieve a highly conformal, silicon-rich, low stress film (~50MPa compressive) that provides good electrical isolation between the center electrode and the surrounding diaphragm. The deposition is followed by a thin LPCVD silicon dioxide deposition, which serves as an etch stop in a downstream etch step. These two dielectric materials are then patterned and etched as shown in Figure 3(a). In order to electrically access the handle layer and use it as the bottom electrode, substrate contact holes are etched

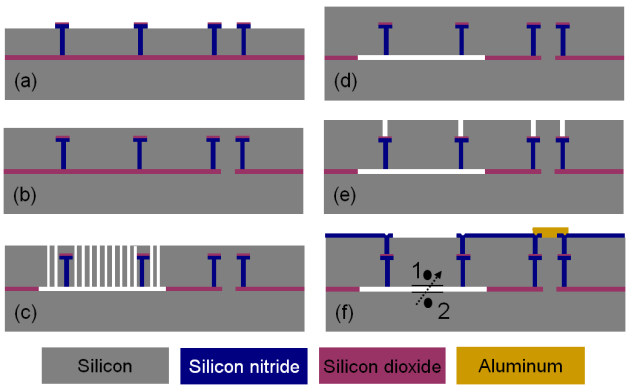

Figure 3: Fabrication process for capacitive pressure sensor with reduced electrode area. (a) Trenches are etched and refilled with nitride; (b) Contact vias are created; (c) Vent holes are etched, followed by a vapor HF release etch; (d) Vent holes are sealed, creating the released membrane; (e) Additional electrical isolation etch is performed; (f) Passivation layer and metal are deposited and etched.

Table 1: List of geometries and performances for three devices.

Device	*Radius* (μm)		*Cnom at 101 kPa* (pF)		*Sensitivity* (fF/kPa)	
	Diaphragm	Electrode	Prediction	Experiment	Prediction	Experiment
D480	240	112.5	1.26	1.44	0.82	0.80
D530	265	150	1.63	1.93	2.31	2.40
D560	280	189.5	2.12	2.50	4.41	4.81

through the SOI device layer, followed by a plasma etch of the exposed buried oxide layer. The electrical via is then created by refilling the contact trench with highly-doped p-type epitaxially grown silicon, as seen in Figure 3(b). Next, the wafer is planarized using chemical-mechanical polishing (CMP) to provide a uniform surface for vent hole lithography. Circular vent hole patterns are etched through the device layer, their placement defining the diaphragm size. This is followed by a vapor phase hydrofluoric (HF) acid release etch, shown in Figure 3(c). An infrared microscope is used to monitor the progress of the oxide etch. Similar to Candler *et al.*, the vent holes are then sealed at high temperature (925 ^{o}C) in an epitaxial silicon reactor [8], providing an ultra clean and low pressure cavity as depicted in Figure 3(d). Another electrode definition trench etch is performed to electrically isolate the electrodes (Figure 3(e)), followed by another silicon nitride deposition to completely fill these trenches.

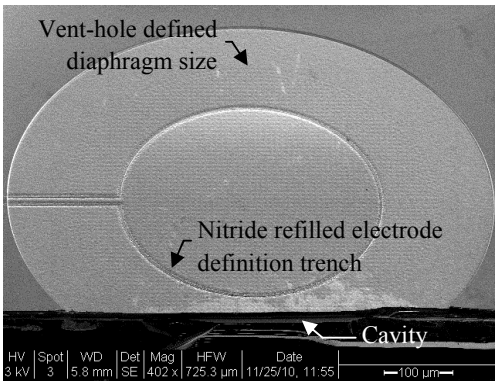

Figure 4: SEM image of a 280 μm radius diaphragm with an electrode radius of 189.5 μm. The diaphragm thickness and cavity gap are 10 μm and 1.5 μm, respectively.

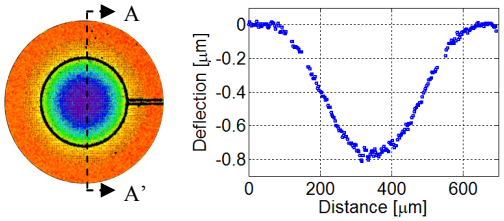

Figure 5: Surface profile of a diaphragm with 265 μm radius measured using Zygo white light interferometery. Left: diaphragm top view. Right: diaphragm deflection across A-A'.

Lastly, the nitride on the topside diaphragm and the contact areas is removed, and the process is finished by sputtering and etching aluminum used for bond pads.

Figure 4 shows an SEM image of a functional capacitive pressure sensor, with the nitride-defined electrode and the vent-hole-defined membrane locations indicated. Figure 5 shows the surface profile of a sealed completed diaphragm measured with a Zygo white light interferometer at atmospheric pressure. The sealed diaphragm has a downward deflection because the internal cavity pressure is on the order of 1 kPa based on the sealing conditions. In order to confirm the cavity is well sealed and not deflected due to film stress, the same device was vented by creating a hole in the center of the diaphragm using a focused ion beam (FIB). After venting the cavity via FIB, there is no pressure difference across the diaphragm, and as a result the diaphragm was observed to return to an undeflected flat state as expected.

SENSOR CHARACTERIZATION

Experimental setup

Table 1 summarizes the geometry of the tested devices. After mounting onto an open cavity package, wire bonding, and soldering to a customized printed circuit board (PCB), the devices are tested in a PFEIFFER vacuum chamber, whose pressure can be controlled by a gas metering valve. An Alpha-Omega Series 800 temperature controller is utilized to drive a thermoelectric cooler for temperature control. A platinum RTD temperature sensor is positioned next to the pressure sensor on the PCB to minimize errors in temperature monitoring. Capacitance is measured by a HP 4285A LCR meter, using appropriate open and short circuit corrections prior to measurement.

Experimental results and discussion

Nominal capacitances at 1 atmosphere (101 kPa) are measured and listed in Table 1 along with their predicted values. The nominal capacitance is a summation of the variable signal capacitance and the parasitic capacitance. Parasitic capacitance is primarily attributed to the

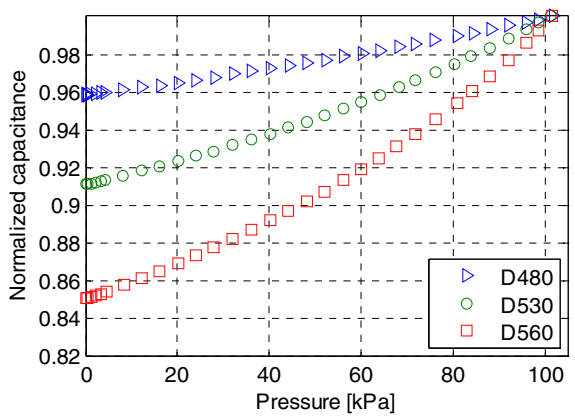

Figure 6: Experimental data of normalized capacitance versus pressure for different sized diaphragms at 25 ºC. Data is normalized by dividing the measured capacitance by C_{nom} at 101 kPa.

capacitance across the nitride filled trench in the device layer defining the top electrode, located at the central portion of the diaphragm and extending to surround the adjacent aluminum bond pad. Although additional sources of stray parasitic capacitance exist, they are considered to be much less significant in magnitude than those noted above. The difference between calculated and measured nominal capacitance (C_{nom} at 101 kPa) can be attributed to the unaccounted for stray capacitance and the fringe capacitance between top and bottom electrodes, which was not included in the theoretical calculation.

When characterizing the sensitivity of the pressure sensors, the vacuum chamber is maintained at 25 ^{o}C to rule out temperature-induced variations. Figure 6 plots the measured capacitance versus pressure for the devices listed in Table 1. Data is normalized using C_{nom}. The performance is also tabulated in Table 1 for ease of comparison. It is found that the device has higher sensitivity than the calculated result and this difference is greater in larger diaphragms. It is believed that the higher value of the experimentally determined sensitivity is caused by process variations and the assumption that the fringe capacitance is negligible. As can be seen from Equations (1) and (2), the diaphragm deflection is proportional to the fourth order of diaphragm radius and inversely proportional to the third order of diaphragm thickness. The timed, vapor HF release step is a potential source of error due to across-wafer uniformity, as are the polishing steps that set the final diaphragm thickness. Improvements regarding both of these process steps have already been determined and should yield improved uniformity and agreement with theory on future devices.

CONCLUSION

We have successfully designed, fabricated, and tested numerous capacitive pressure sensors with reduced electrode size. Owing to the ultra-clean cavity and precise gap control, the preliminary experimental results match the design targets within the error associated with certain processing steps. The electrode-size tuning feature adds an additional design knob that helps alleviate readout circuitry design complexity by improving fractional capacitance change.

ACKNOWLEDGMENTS

This project is funded by Robert Bosch LLC, Research and Technology Center in Palo Alto, CA. The fabrication is carried out in the Stanford Nanofabrication Facility. The authors would also like to thank C.-J. Chung for her assistance during device characterization.

REFERENCES

[1] W.P. Eaton and J.H. Smith, "Micromachined Pressure Sensors: Review and Recent Developments," *Smart Mater. Struct.*, vol. **6**, pp. 530–539, 1997.

[2] A.V. Chavan and K.D. Wise, "Batch-Processed Vacuum-Sealed Capacitive Pressure Sensors," *JMEMS*, vol. **10**, pp. 580–588, 2001.

[3] S.D. Senturia, "Microsystem Design," 1st edition, Kluwer Academic Publishers, 2001.

[4] J.B. Nysather *et al.*, "Measurement of package-induced stress and thermal zero shift in transfer molded silicon piezoresistive pressure sensors," *JMEMS*, vol. 8, pp. 168–171, 1998.

[5] R.H. Krondorfer and Y.K. Kim, "Packaging Effect on MEMS Pressure Sensor Performance," *Transactions on Components and Packaging Technologies*, vol. **30**, pp. 285–293, 2007.

[6] B. Kim *et al.*, "Using MEMS to Build the Device and the Package," *Transducers'07 Conference*, *Lyon, France*, June 10-14, 2007, pp.331–334.

[7] S.P. Timoshenko, "Theory of Plates and Shells," New York: McGraw Hill, 1959

[8] R.N. Candler *et al.*, "Long-Term and Accelerated Life Testing of a Novel Single-Wafer Vacuum Encapsulation of MEMS Resonators," *JMEMS*, vol. **15**, pp. 1446–1456, 2006.

CONTACT

Chia-Fang Chiang, e-mail: cfchiang@mems.stanford.edu